Journal of Power Sources 254 (2014) 218–223

Contents lists available at ScienceDirect

Journal of Power Sources

journal homepage: www.elsevier.com/locate/jpowsour

Characterization and kinetic study of a nanostructured rhodium electrode for the hydrogen oxidation reaction

María A. Montero, José L. Fernández, María R. Gennero de Chialvo, Abel C. Chialvo*

Programa de Electroquímica Aplicada e Ingeniería Electroquímica (PRELINE), Facultad de Ingeniería Química, Universidad Nacional del Litoral, Santiago del Estero 2829, 3000 Santa Fe, Argentina

HIGHLIGHTS

- Preparation and characterization of nanostructured rhodium electrodes.
- Kinetic study of the hydrogen oxidation reaction.
- Correlation of experimental results through a unique set of kinetic parameters.
- Reaction takes place under both Tafel–Volmer and Heyrovsky–Volmer routes.

ARTICLE INFO

Article history:
Received 15 October 2013
Received in revised form
19 December 2013
Accepted 20 December 2013
Available online 30 December 2013

Keywords:
Rhodium electrode
Hydrogen oxidation reaction
Kinetic parameters
Exchange current density

ABSTRACT

The hydrogen oxidation reaction was studied on a nanostructured rhodium electrode at different rotation rates. The electrode was prepared via sputtering on a glassy carbon disc support and it was characterized by X-ray Photoelectron Spectroscopy (XPS), Atomic Force Microscopy (AFM) and cyclic voltammetry, which allowed verifying the nanostructured morphology and the absence of any phase other than metallic rhodium. The real surface area was evaluated by CO stripping voltammetry. Experimental current density (j) – overpotential (η) curves of the hydrogen oxidation reaction were obtained in the range $-0.015\ V \leq \eta \leq 0.25\ V$ at different rotation rates in sulphuric acid solution. They were correlated by kinetic expressions derived from the Tafel–Heyrovsky–Volmer mechanism and thus the kinetic parameters were evaluated. It was verified that over this overpotential region the reaction proceeds through the simultaneous occurrence of the Tafel–Volmer and the Heyrovsky–Volmer route.

1. Introduction

The hydrogen oxidation reaction (*hor*) has received considerable attention in relation to the development of the H_2–O_2 proton exchange membrane fuel cell (PEMFC) [1]. Therefore, the elucidation of the factors that define the electrocatalytic behaviour for this reaction is essential for the development of new and cheaper electrode materials. Kinetic studies of the hydrogen electrode reaction have been carried out on different metals preferably in the cathodic overpotentials range, which corresponds to the hydrogen evolution reaction (*her*) [2]. Starting from these results, it has been established that platinum has the highest electrocatalytic activity, as it can be derived from its position on the top of the volcano curve, which relates the exchange current density (j_o) with the adsorption free energy of the reaction intermediate [3–6]. On the other hand, the number of kinetic studies of the *hor* is significantly less, most of them carried out on Pt, on smooth electrodes [7–10] as well as on supported nanoparticles [11–13]. Among the scarce kinetic data of the *hor* on other noble metals, it can be cited the evaluation of the kinetic parameters on Pd [14,15], Ru [16] and Ir [17].

There are only a few studies of the hydrogen electrode reaction on rhodium. The first antecedent corresponds to an evaluation of the equilibrium polarization resistance [18]. Another work measured the exchange current density and the Tafel slope (b) for the *hor* as a function of hydrogen partial pressure [19]. These experimental kinetic parameters were also measured for the *her* on acid solution [20]. More recently this reaction was studied by faradaic impedance, including the hydrogen absorption process [21]. Therefore, there has been no report about kinetic studies of the hydrogen oxidation reaction on Rh electrodes. On this context, the present work deals with the evaluation of the elementary kinetic parameters of the Volmer-Heyrovsky-Tafel mechanism on nanostructured Rh electrodes through the correlation of experimental current density (j) vs. overpotential (η) curves, measured in

* Corresponding author. Tel.: +54 342 457 1164x2519; fax: +54 342 4536861.
E-mail address: achialvo@fiq.unl.edu.ar (A.C. Chialvo).

0378-7753/$ – see front matter © 2014 Elsevier B.V. All rights reserved.
http://dx.doi.org/10.1016/j.jpowsour.2013.12.095

sulphuric acid solution under steady state and controlled mass transport conditions.

2. Experimental details

2.1. Electrode preparation

The working electrodes were prepared via sputtering on a glassy carbon (GC) substrate from a rhodium target provided by Goodfellow Corp. in an argon atmosphere (0.1 mbar), using a sputter coater Emitech K500X, operated at 30 mA during 4 min. Previously to Rh deposition, the glassy carbon (SPI-Glas^{TM} 25) substrate was mirror polished and subjected to ultrasonic cleaning in ultrapure water for 5 min and then was voltammetrically characterized to ensure a clean and reproducible deposition surface.

2.2. Electrode characterization

The surface morphology of the Rh electrodes was characterized by Atomic Force Microscopy (AFM). AFM images were obtained using a multi-technique Agilent microscope model 5400, operated in tapping mode and processed with the software WSxM 6.2.

The Rh electrode was also physicochemically characterized by X-ray Photoelectron Spectroscopy (XPS) using a multitechnique system (SPECS) equipped with a dual Mg/Al X-ray source and a hemispherical PHOIBOS 150 analyzer operating in the fixed analyzer transmission (FAT) mode. The spectra were obtained with pass energy of 30 eV; a Mg Ka X-ray source was operated at 200 W and 12 kV. The working pressure in the analysing chamber was less than 5.9×10^{-7} Pa. The XPS analyses were performed in the spectral region corresponding to Rh 3d core level. The data treatment was performed with the Casa XPS program (Casa Software Ltd., UK).

2.3. Electrochemical measurements

All the electrochemical measurements were performed in a three electrodes cell specially built for the use of a rotating electrode and with a particular design of the gas saturator at 298 K. The electrolytic solution was 0.5 M H_2SO_4, prepared with ultra-pure water (PureLab, Elga LabWater). The working electrode was mounted in a teflon holder, with an exposed geometric area of 0.07 cm^2. It was rotated through the use of a rotating disk Radiometer EDI 10K system. Furthermore, a large area platinum wire acted as counter electrode and a hydrogen electrode in the same solution (RHE) was used as reference electrode. The working electrode was electrochemically characterized by cyclic voltammetry using a potentiostat-galvanostat Wenking POS2 controlled by an interface Advantech PI1710HG and the software Labview 8. The voltammograms were obtained at 0.1 V s^{-1} in nitrogen saturated solution between 0.0 and 1.3 V.

The electrocatalytic activity towards the hydrogen oxidation reaction was evaluated through the current (I) – overpotential (η) response in hydrogen saturated solution. The polarization curves were obtained at different rotation rates in the range $900 \leq \omega/\text{rpm} \leq 4900$. A potential program was applied, which initiated with a 3 s step at 0.0 V, followed by a 5 s step to the desired overpotential value. In this last period, readings of the current value were made each 0.1 s and the mean value of the current data measured in the last 2 s was assigned to the step overpotential. Then the program was repeated for each η value, which was varied in the range $-0.015 \leq \eta/\text{V} \leq 0.25$. The electrolyte solution was renewed after each experiment.

Finally, the real area of the electrode was determined by CO stripping voltammetry. CO adsorption was carried out in an auxiliary cell in a CO saturated solution, holding the electrode potential at 0.05 V during 15 min. Then, the voltammetric stripping was carried out at 0.05 V s^{-1} in nitrogen saturated solution between 0.0 and 1.3 V.

3. Results and discussion

3.1. Morphological and physicochemical characterization

The surface morphology was analysed by AFM (Fig. 1). It can be observed that the Rh layer, deposited by sputtering on a glassy carbon substrate, consists of uniformly distributed nanoparticles. In order to estimate the particle size, the height profile was analysed in different places on the electrode surface. Two of them are illustrated in the inset of Fig. 1. The average height of the nanoparticles obtained from these profiles is ranging between 2 and 6 nm.

The physicochemical characterization of the Rh electrode was carried out by XPS analysis. Fig. 2 illustrates the spectrum in the range of binding energy comprised between 303 and 318 eV (continuous line). It can be observed two peaks located at 307.0 eV and 311.8 eV respectively, which are in agreement with the values reported for $3d_{5/2}$ and $3d_{3/2}$ signals of metal rhodium [22]. The deconvolution of these peaks is also shown (dotted lines).

3.2. Electrochemical characterization and real area evaluation

Fig. 3 shows the voltammetric profile of the nanostructured Rh electrode obtained in 0.5 M H_2SO_4 solution at 0.05 V s^{-1} under nitrogen bubbling. The electrode was previously subjected to a CO adsorption carried out in an auxiliary cell in a CO saturated solution at 0.05 V during 15 min. The first cycle corresponds to the stripping of the adsorbed CO, where it can be observed a sharp peak at approximately 0.725 V. The complete electrooxidation of the adsorbed CO is produced in this first anodic sweep, as it can be verified through the second voltammetric cycle, which reproduces the blank voltammogram of metallic rhodium in this electrolyte

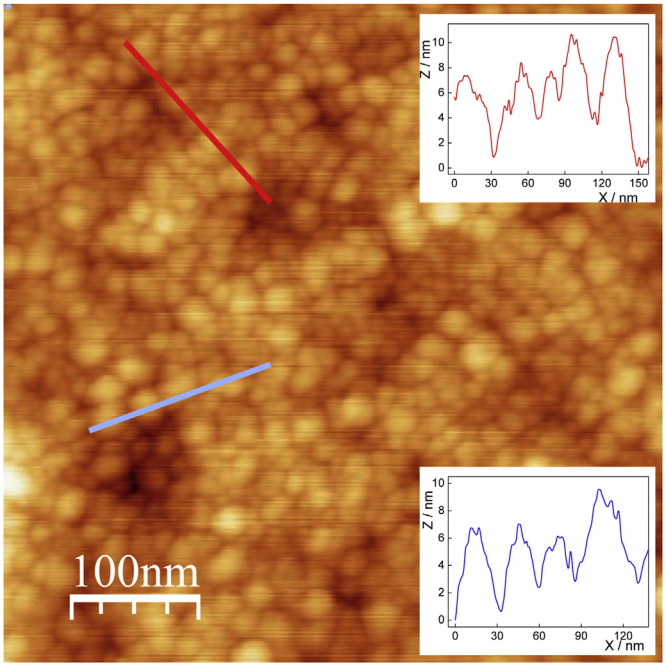

Fig. 1. AFM image of the nanostructured Rh electrode. Insets: height profiles.

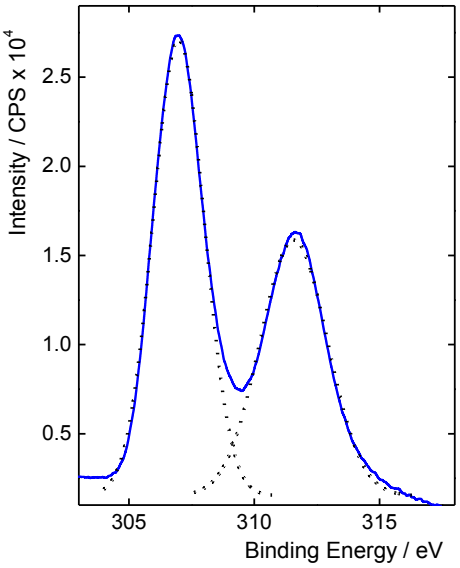

Fig. 2. XPS Rh *3d* spectra of the nanostructured Rh electrode (continuous line) and deconvolution of the peaks (dotted lines).

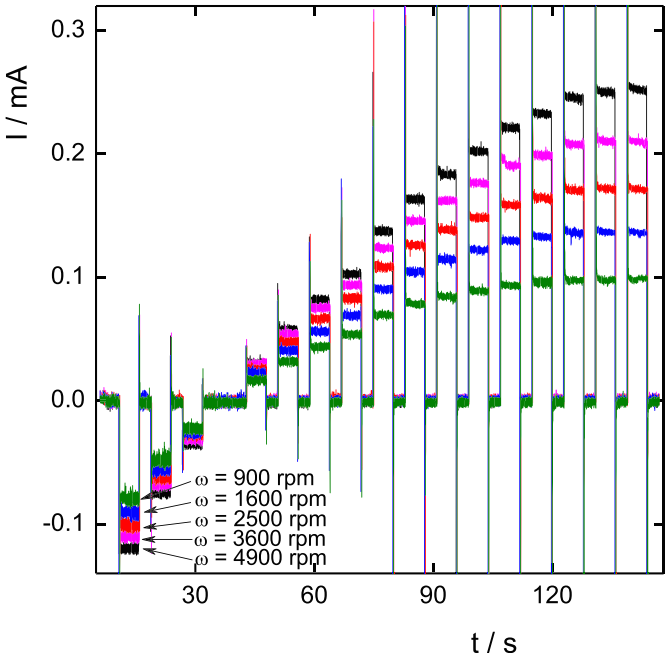

Fig. 4. Current vs. time response of Rh electrode to the overpotential program applied in the range $-0.015\ V \leq \eta \leq 0.25\ V$ at different rotation rates (indicated in the figure). 0.5 M H_2SO_4; 298 K.

solution. It can be appreciated that the voltammetric profile, and in particular the potential region where the hydrogen adsorption takes place, is very similar to those found in the literature [23,24]. Moreover, this result is in agreement with the XPS analysis, where only metallic rhodium was found.

The voltammetric charge corresponding to the electro-oxidation of the adsorbed CO was used for the determination of the real electrode area. This charge was evaluated as the difference between the first and second cycle in the potential range $0.40 < E/V < 1.3$, resulting a value equal to 110.5 μC. Taking into account that for Pt [25], Pd [26] and Ir [17], the surface coverage corresponding to the CO saturation is 66% of the total surface sites, it should be reasonable to consider that this value is also applicable for the case of Rh. On this basis, the voltammetric charge of one CO monolayer is equal to 287.7 μC cm^{-2} and

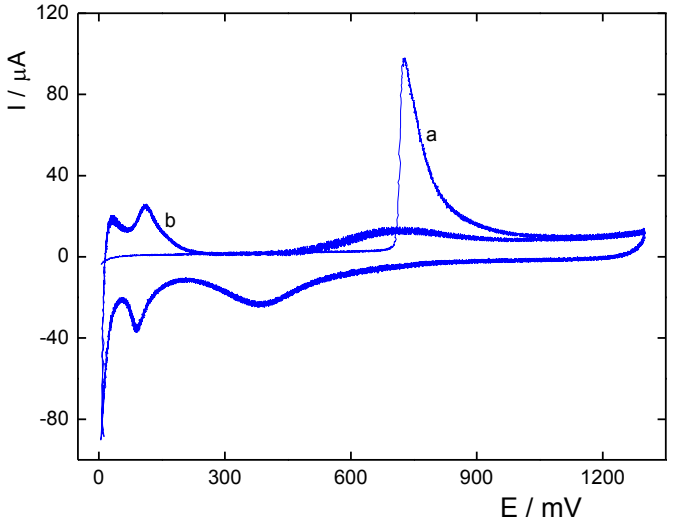

Fig. 3. Voltammogram of the Rh electrode after CO adsorption. (a) First cycle; (b) Second cycle. 0.05 V s^{-1}; 0.5 M H_2SO_4, 298 K.

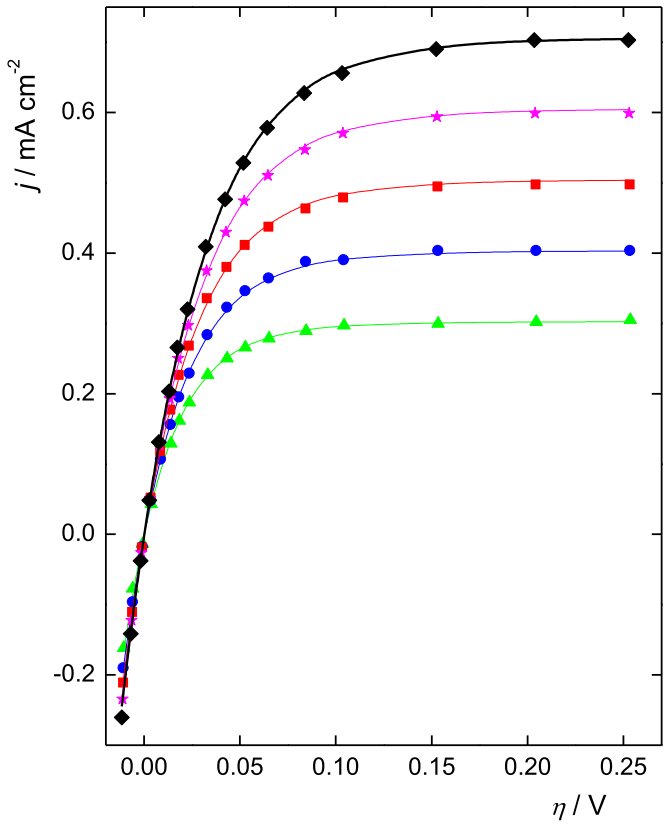

Fig. 5. Experimental (symbols) and simulated (lines) $j(\eta)$ curves of the *hor* on Rh electrode. 0.5 M H_2SO_4; 298 K. ω = (▲) 900; (●) 1600; (■) 2500; (★) 3600; (◆) 4900 rpm.

therefore the real area of the Rh electrode is 0.384 cm^2. Moreover, as the reaction under study has a strong diffusion contribution, which depends on the geometric area, meanwhile the kinetic reaction takes place on the real surface area, the relationship between both values is an important parameter for the correct analysis of the reaction. This relationship, called active area factor (f_{aa}), is in this case equal to 5.486. It appears in the kinetic equations for the hydrogen oxidation reaction (item 3.3).

3.3. Hydrogen oxidation reaction

The evaluation of the experimental dependence current (I) vs. η for the hydrogen oxidation reaction on a nanostructured Rh electrode was carried out in 0.5 M H_2SO_4 solution under hydrogen bubbling at different rotation rates ($900 \leq \omega/\text{rpm} \leq 4900$). After the open circuit potential reached the equilibrium value (0.0 ± 0.0004 V vs. RHE), a potential program was applied, which initiated with a 3 s step at 0.0 V, followed by a 5 s step to the desired overpotential value. Then the program was repeated for each η value, which was varied in the range $-0.015 \leq \eta/\text{V} \leq 0.25$. The current on time ($t$) response of the Rh electrode resulting from the application of the potential program is shown in Fig. 4, for all the rotation rates analysed (900, 1600, 2500, 3600 and 4900 rpm). It can be observed that current quickly reached the steady state condition. Readings of the current value were made each 0.1 s and the mean value of the current data measured in the last 2 s was assigned to the step overpotential. Starting from these results and taking into account the real electrode area, the corresponding $j(\eta)$ dependences on steady state were evaluated for each rotation rate, which are shown in Fig. 5 (symbols). These experimental curves were correlated with the system of equations resulting from the resolution of the kinetic mechanism of Tafel–Heyrovsky–Volmer on steady state, which is valid for the hydrogen electrode reaction on a metallic surface. The corresponding steps can be written as,

$$H_2 + 2S \rightleftarrows 2H_{ad} \quad \text{Tafel} \tag{1a}$$

$$H_2 + S \rightleftarrows H_{ad} + H^+ + e^- \quad \text{Heyrovsky} \tag{1b}$$

$$H_{ad} \rightleftarrows H^+ + e^- + S \quad \text{Volmer} \tag{1c}$$

where S represents a site on the electrode surface in which the reaction intermediate H_{ad} can be adsorbed. The experimental dependences $j(\eta, \omega)$ were described with the kinetic expression resulting from the rigorous resolution of the kinetic mechanism on steady state, considering a Frumkin type adsorption of the reaction intermediate. Details of the resolution, which considers the simultaneous occurrence of the two independent routes, Tafel-Volmer and Heyrovsky-Volmer, can be found elsewhere [[27] and references cited there]. Three equivalent expressions for $j(\eta, \omega)$ are derived, referred to the real or active area, resulting from the mass balance in steady state. The equation used in the present work was,

$$j(\eta,\omega) = \frac{v_H^e e^{-u(\theta-\theta^e)\lambda} e^{\alpha_H f\eta}\left[\frac{(1-\theta)}{(1-\theta^e)} - \frac{\theta e^{-f\eta} e^{u(\theta-\theta^e)}}{\theta^e}\right] + v_T^e e^{-2u(\theta-\theta^e)\lambda}\left[\frac{(1-\theta)^2}{(1-\theta^e)^2} - \frac{\theta^2 e^{2u(\theta-\theta^e)}}{\theta^{e2}}\right]}{\frac{1}{2F} + \frac{v_T^e f_{aa}(1-\theta)^2 e^{-2u(\theta-\theta^e)\lambda}}{B\omega^{1/2}(1-\theta^e)^2} + \frac{v_H^e f_{aa}(1-\theta) e^{-u(\theta-\theta^e)\lambda} e^{\alpha_H f\eta}}{B\omega^{1/2}(1-\theta^e)}} \tag{2}$$

The implicit equation for the variation of the surface coverage (θ) of the reaction intermediate on overpotential is given by,

$$\left\{ v_V^e e^{-u(\theta-\theta^e)\lambda} e^{\alpha_V f\eta}\left[\frac{\theta e^{u(\theta-\theta^e)}}{\theta^e} - \frac{(1-\theta)e^{-f\eta}}{(1-\theta^e)}\right] + v_H^e e^{-u(\theta-\theta^e)\lambda} e^{\alpha_H f\eta} \left[\frac{(1-\theta)}{(1-\theta^e)} - \frac{\theta e^{-f\eta} e^{u(\theta-\theta^e)}}{\theta^e}\right]\right\} \times \left\{\frac{1}{2F} + \frac{v_T^e f_{aa}(1-\theta)^2 e^{-2u(\theta-\theta^e)\lambda}}{B\omega^{1/2}(1-\theta^e)^2}\right\} - \left\{\frac{1}{F} + \frac{v_H^e f_{aa}(1-\theta) e^{-u(\theta-\theta^e)\lambda} e^{\alpha_H f\eta}}{B\omega^{1/2}(1-\theta^e)}\right\} \times \left\{ v_V^e e^{-u(\theta-\theta^e)\lambda} e^{\alpha_V f\eta}\left[\frac{\theta e^{u(\theta-\theta^e)}}{\theta^e} - \frac{(1-\theta)e^{-f\eta}}{(1-\theta^e)}\right] - v_T^e e^{-2u(\theta-\theta^e)\lambda}\left[\frac{(1-\theta)^2}{(1-\theta^e)^2} - \frac{\theta^2 e^{2u(\theta-\theta^e)}}{\theta^{e2}}\right]\right\} = 0 \tag{3}$$

In equations (2) and (3), v_i is the reaction rate of the step i ($i = T$, H, V), α_i ($i = V$, H) is the symmetry factor of the step i, λ is the symmetry factor of adsorption, u (in RT units) is the energy of interaction between the adsorbed hydrogen atoms and B is the Levich constant. Superscript e indicates equilibrium and $f = F/RT$. The experimental $j(\eta)$ curves for each ω value can be correlated using equations (2) and (3), applying a non linear least squares regression method. However, it is necessary first to evaluate the value of constant B. The relationship f_{aa}/B can be evaluated from the values of the maximum current (j_{max}) observed for $\eta > 0.20$ V, as it is related to the rotation rate as follows [28],

$$\frac{1}{j_{max}(\omega)} = \frac{1}{j_{max}^{kin}} + \left(\frac{f_{aa}}{B}\right)\frac{1}{\omega^{1/2}} \tag{4}$$

where j_{max}^{kin} is the limiting kinetic current density of the Tafel step, which represents the mixed behaviour of the hydrogen oxidation, with simultaneous kinetic and diffusion contributions. It is given by the following expression [28],

$$j_{max}^{kin} = \frac{2Fv_T^e e^{2\lambda u\theta^e}}{(1-\theta^e)^2} \tag{5}$$

Therefore, the constants f_{aa}/B and j_{max}^{kin} can be obtained from the slope and the origin ordinate of the experimental plot j_{max}^{-1} vs. $\omega^{-1/2}$. Fig. 6 illustrates such plot, where it can be observed that the experimental points (dots) satisfy the required linearity. From linear regression (line) the following values were obtained: $f_{aa}/B = 99.129\ \text{mA}^{-1}\,\text{cm}^2\,\text{rpm}^{1/2}$ and $(j_{max}^{kin})^{-1} = 0.02707\ \text{mA}^{-1}\,\text{cm}^2$. The following relationship between the parameters v_T^e and θ^e is also obtained from equation (5),

$$v_T^e\left[\text{mol}\,\text{cm}^{-2}\text{s}^{-1}\right] = 1.914\,10^{-7}(1-\theta^e)^2 e^{-2u\theta^e} \tag{6}$$

Then, the experimental dependences $j(\eta, \omega)$ were correlated using equations (2), (3) and (6), applying a non linear least squares

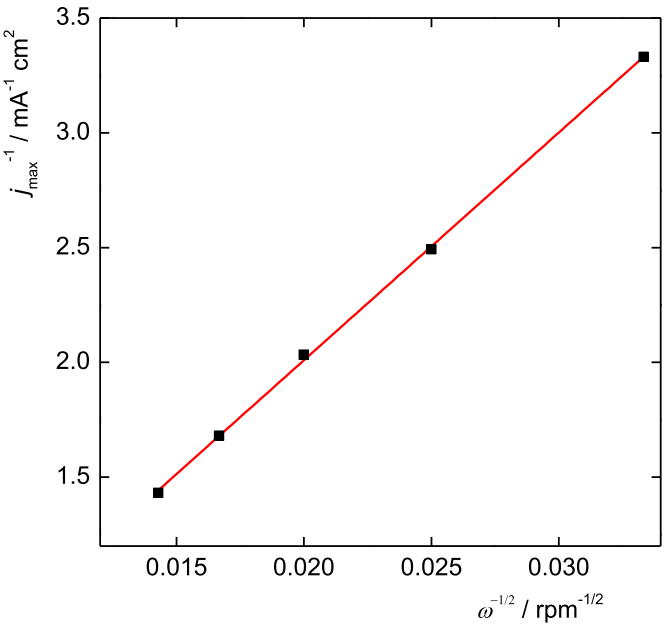

Fig. 6. j_{max}^{-1} vs. $\omega^{-1/2}$ plot. Experimental (symbols), linear regression (line).

regression method carried out with the software Micromath Scientific 3.0, considering the symmetry factors $\alpha_V = \alpha_H = \lambda = 0.5$. The kinetic parameters $\nu_V^e, \nu_H^e, \theta^e$ and u were evaluated from the correlation and the value of ν_T^e was obtained from equation (6). Each polarization curve corresponding to a particular rotation rate was correlated independently. The minimization of the mean squared error led for all the rotation rates to the cancellation of the interaction parameter u, which means that the adsorption of the reaction intermediate follows a Langmuir isotherm. The values of the kinetic parameters ν_V^e, ν_H^e and θ^e as well as the corresponding mean values are shown in Table 1.The simulations of the dependences $j(\eta, \omega)$ were done with this unique set of parameters, which are shown in Fig. 5 (lines). It can be appreciated that there is a good agreement between the experimental and simulated curves and that in the analysed potential range the hydrogen oxidation is verified through both, Tafel-Volmer and Heyrovsky–Volmer routes, being the two contributions significant.

3.4. Electrocatalytic activity

As it was already mentioned, the electrocatalytic activity of a given electrode material for the hydrogen electrode reaction is represented in the volcano curve by the exchange current density, which is related to the kinetic parameters by the following equation [29],

$$j_o = 2F\left(\frac{\nu_T^e\nu_V^e + \nu_H^e\nu_V^e + \nu_T^e\nu_H^e}{(\nu_V^e + \nu_H^e + 2\nu_T^e)}\right) \quad (7)$$

The value obtained from the data given in Table 1 (0.677 mA cm^{-2}), is slightly higher than that mentioned in the literature (0.316 mA cm^{-2}) [30]. It is also almost two orders of magnitude lower than that corresponding to Pt nanoparticles supported on GC (45.9 mA cm^{-2}) [11].

Moreover, the equilibrium polarization resistance (R_p^o) can be also evaluated from the kinetic parameters [29],

$$R_p^o = \frac{RT}{4F^2}\left(\frac{4\nu_T^e + \nu_H^e + \nu_V^e}{\nu_T^e\nu_V^e + \nu_H^e\nu_V^e + \nu_T^e\nu_H^e}\right) \quad (8)$$

The resulting value is $R_p^o = 38.6\ \Omega\ cm^2$, which is higher than that reported by J.P. Hoare and S. Schuldiner (25.0 Ω cm^2) [18]. However, it can be appreciated in Fig. 1 of such reference that the dependence $j(\eta)$ is not linear and that from the tangent line at the origin the value $R_p^o = 44.0\ \Omega\ cm^2$ is obtained, which is more in agreement with the present result. As it is expected, this value is also significantly higher than that on Pt (0.355 Ω cm^2) [11].

Table 1
Kinetic parameters for the *hor* at different rotation rates.

Kinetic parameters	Rotation rate/rpm					Mean value
	900	1600	2500	3600	4900	
$\nu_T^e \times 10^9$/mol cm^{-2} s^{-1}	1.340	1.318	1.277	1.059	1.295	1.257
$\nu_H^e \times 10^9$/mol cm^{-2} s^{-1}	5.949	5.766	6.073	6.457	6.169	6.083
$\nu_V^e \times 10^8$/mol cm^{-2} s^{-1}	5.546	5.546	5.546	5.546	5.546	5.546
θ^e	0.464	0.456	0.465	0.458	0.466	0.462

4. Conclusions

The hydrogen oxidation reaction was studied on a rotating disc electrode of nanostructured rhodium supported on glassy carbon, being the electroactive area evaluated by CO stripping voltammetry. The kinetic parameters resulting from the rigorous resolution of the Tafel-Heyrovsky-Volmer mechanism were evaluated from the correlation of the experimental current density–overpotential curves measured at different rotation rates. It was demonstrated that in the analysed overpotential region the reaction takes place through the Tafel–Volmer route and the Heyrovsky–Volmer route. It was found that both contributions are significant and that there is no prevalence of one route over the other. Self consistent values of the exchange current density and the equilibrium polarization resistance of the hydrogen electrode reaction were also evaluated from these kinetic parameters. These results were discussed and compared with values reported in the literature.

Acknowledgements

The authors wish to acknowledge the financial support received from ANPCyT, CONICET and UNL. Thanks are also given to ANPCyT for the purchase of the SPECS multitechnique analysis instrument (PME2003-8).

References

[1] J. Zang (Ed.), PEM Fuel Cell Electrocatalysts and Catalyst Layers. Fundamentals and Applications, Springer Verlag, London, 2008.
[2] E. Santos, A. Lundin, K. Potting, P. Quaino, W. Schmickler, Phys. Rev. B 79 (2009) 235436.
[3] S. Trasatti, J. Electroanal. Chem. 39 (1972) 163–184.
[4] O.A. Petrii, G.A. Tsirlina, Electrochim. Acta 39 (1994) 1739–1747.
[5] J.K. Norskov, T. Bligaard, A. Logodottir, J.G. Chen, S. Pandelov, U. Stimming, J. Electrochem. Soc. 152 (2005) J23–J26.
[6] W. Sheng, M.N.Z. Myint, J.G. Chen, Y. Yan, Energy Environ. Sci. 6 (2013) 1509–1512.
[7] N.M. Markovic, B.N. Grgur, P.N. Ross, J. Phys. Chem. C. 101 (1997) 5405–5413.
[8] P.M. Quaino, M.R. Gennero de Chialvo, A.C. Chialvo, Phys. Chem. Chem. Phys. 6 (2004) 4450–4455.
[9] K. Kunimatsu, H. Uchida, M. Osawa, M. Watanabe, J. Electroanal. Chem. 587 (2006) 299–307.
[10] R. Kajiwara, Y. Asaumi, M. Nakamura, N. Hoshi, J. Electroanal. Chem. 657 (2011) 61–65.
[11] M.A. Montero, M.R. Gennero de Chialvo, A.C. Chialvo, Electrochem. Commun. 12 (2010) 398–401.
[12] Y. Sun, Y. Dai, S. Chen, Phys. Chem. Chem. Phys. 14 (2012) 2278–2285.
[13] I. Esparbé, E. Brillas, F. Centellas, J.A. Garrido, R.M. Rodríguez, C. Arias, P.L. Cabot, J. Power Sources 190 (2009) 201–209.
[14] S.N. Pronkin, A. Bonnefont, P.S. Ruvinskiy, E.R. Savinova, Electrochim. Acta 55 (2010) 3312–3323.
[15] M.S. Rau, P.M. Quaino, M.R. Gennero de Chialvo, A.C. Chialvo, Electrochem. Commun. 10 (2008) 208–212.

[16] M.S. Rau, M.R. Gennero de Chialvo, A.C. Chialvo, Electrochim. Acta 55 (2010) 5014–5018.
[17] M.A. Montero, J.L. Fernandez, M.R. Gennero de Chialvo, A.C. Chialvo, J. Phys. Chem. C. 117 (2013) 25269–25275.
[18] J.P. Hoare, S. Schuldiner, J. Chem. Phys. 25 (1956) 786.
[19] S. Schuldiner, J. Electrochem. Soc. 107 (1960) 452–457.
[20] J.O'M. Bockris, S. Srinivasan, Electrochim. Acta 9 (1964) 31–44.
[21] V. Horvat-Radosevic, K. Kvastek, Electrochim. Acta 48 (2002) 311–322.
[22] L. Marot, G. De Temmerman, V. Thommen, D. Mathys, P. Oelhafen, Surf. Coat. Technol. 202 (2008) 2837–2843.
[23] B. Losiewicz, R. Jurczakowski, A. Lasia, Electrochim. Acta 56 (2011) 5746–5753.
[24] X.F. Lin, B. Ren, Z.Q. Tian, J. Phys. Chem. B 108 (2004) 981–986.
[25] Z. Jusys, T.J. Schmidt, L. Dubau, K. Lasch, L. Jörissen, J. Garche, R.J. Behm, J. Power Sources 105 (2002) 297–304.
[26] L. Fang, Q. Tao, M. Li, L. Liao, D. Chen, Y. Chen, Chin. J. Phys. Chem. 23 (2010) 543–548.
[27] M.A. Montero, M.R. Gennero de Chialvo, A.C. Chialvo, Electrochim. Acta 56 (2010) 731–738.
[28] M.S. Rau, M.R. Gennero de Chialvo, A.C. Chialvo, J. Power Sources 229 (2013) 210–215.
[29] M.R. Gennero de Chialvo, A.C. Chialvo, J. Electroanal. Chem. 415 (1996) 97–106.
[30] S. Trasatti, J. Electroanal. Chem. 39 (1972) 163–183.